Influence of Synthetic and Processing Parameters on the Surface Area, Speciation, and Particle Formation in Copper Oxide/Silica Aerogel Composites

Jaya L. Mohanan and Stephanie L. Brock*

Department of Chemistry, Wayne State University, Detroit, Michigan 48202

Received November 25, 2002. Revised Manuscript Received April 4, 2003

A systematic study of the effects of pH, precursor salt, and temperature on the surface area, particle size, and copper speciation in 3 wt % CuO in silica aerogels and xerogels has been conducted. The materials were synthesized by copolymerization sol−gel reactions, followed by either supercritical solvent extraction using CO_2 (aerogels) or conventional drying (xerogels) and annealing in air. Among the six different copper precursors examined, copper(II) acetate was found to be the best in terms of its stability, solubility, and binding capacity of copper in the silica matrix. Aerogels prepared with copper(II) acetate were found to have considerably higher surface areas than the corresponding xerogels, and the observed formation of CuO particles occurred at higher temperatures (900 vs 650 °C, by TEM analysis). X-ray diffraction of gels annealed at 900 °C likewise revealed the presence of nanocrystalline CuO, with larger particles observed in acid-catalyzed aerogels vs base-catalyzed aerogels (∼26 vs ∼15 nm, respectively). Additionally, in 900 °C annealed acid- and base-catalyzed xerogels, the silica matrix crystallized as crystobalite and quartz, respectively. EPR data suggest that the Cu^{2+} environment goes through a series of structural changes upon annealing. These changes are significantly different in acid- vs base-catalyzed systems because of differences in the internal structures and pore distributions of the materials. In both cases, a broad isotropic component, attributed to CuO, is observed upon heating. By 900 °C, the hyperfine peaks originally attributed to dispersed Cu^{2+} are absent in base-catalyzed systems, but they are still present as a small fraction in acid-catalyzed systems, suggesting incomplete transformation in the latter case.

Introduction

Aerogels are inorganic polymers (typically silica-based) that are synthesized by supercritical drying of swollen gels, themselves produced via sol−gel reactions. They feature high surface areas, low densities, and a combination of micro- and mesoporosity.[1−5] As such, pure silica aerogels have the potential for a wide variety of applications as sensor or catalyst supports, thermal insulators, and dielectrics.[6−9] The range and viability of aerogel applications can be effectively increased by doping a reactive component into the silica aerogel, thereby altering the electrical, magnetic, catalytic, or other physical properties, as appropriate.[7,10−17] Examples include deposition of ruthenium dioxide on the internal surface of a silica aerogel to produce an electrically conductive aerogel,[10] copolymerization of fluorescent molecules with silica to form aerogel oxygen sensors,[18] and covalent attachment of ruthenium phosphine complexes to silica aerogels to produce a heterogeneous catalyst for the formation of formic acid derivatives.[19]

Copper/silica composites are efficient catalysts for a number of processes, including the hydrogenation of alkynes to alkenes[20,21] and the dehydrogenation of alcohols.[22,23] The activity, selectivity, and resistance to deactivation depend on the microstructural properties

(1) Fricke, J. *Sci. Am.* **1988**, *258*, 92−97.
(2) Mehrotra, R. C. *J. Non-Cryst. Solids* **1992**, *145*, 1−10.
(3) Hüsing, N.; Schubert, U. *Angew. Chem., Int. Ed.* **1998**, *37*, 22−45.
(4) Hrubesh, L. W. *J. Non-Cryst. Solids* **1998**, *225*, 335−342.
(5) Leventis, N.; Sotiriou-Leventis, C.; Zhang, G.; Rawashdeh, A. M. *Nano Lett.* **2002**, *2*, 957−960.
(6) Fricke, J.; Tillotson, T. *Thin Solid Films* **1997**, *297*, 212−223.
(7) Pajonk, G. M. *Catal. Today* **1997**, *35*, 319−337.
(8) Anderson, M. T.; Sawyer, P. S.; Rieker, T. *Microporous Mesoporous Mater.* **1998**, *20*, 53−65.
(9) Tillotson, T. M.; Hrubesh, L. W. *J. Non-Cryst. Solids* **1992**, *145*, 44−50.
(10) Rolison, D. R.; Dunn, B. *J. Mater. Chem.* **2001**, *11*, 963−980.
(11) Morris, C. A.; Anderson, M. L.; Stroud, R. M.; Merzbacher, C. I.; Rolison, D. R. *Science* **1999**, *284*, 622−624.
(12) Merzbacher, C. I.; Barker, J. G.; Long, J. W.; Rolison, D. R. *Nanostruct. Mater.* **1999**, *12*, 551−554.
(13) Anderson, M. L.; Morris, C., A.; Stroud, R., M.; Merzbacher, C. I.; Rolison, D. R. *Langmuir* **1999**, *15*, 674−681.
(14) Hair, L. M.; Owens, L.; Tillotson, T.; Froba, M.; Wong, J.; Thomas, G. J.; Medlin, D. L. *J. Non-Cryst. Solids* **1995**, *186*, 168−176.
(15) Buckley, A. M.; Greenblatt, M. *J. Non-Cryst. Solids* **1992**, *146*, 97−110.
(16) Owens, L.; Tillotson, T. M.; Hair, L. M. *J. Non-Cryst. Solids* **1995**, *186*, 177−183.
(17) Hunt, A. J.; Ayers, M. R.; Cao, W. *J. Non-Cryst. Solids* **1995**, *185*, 227−232.
(18) Leventis, N.; Elder, I. A.; Rolison, D. R.; Anderson, M. L.; Merzbacher, C. I. *Chem. Mater.* **1999**, *11*, 2837−2845.
(19) Schmid, L.; Rohr, M.; Baiker, A. *Chem. Commun.* **1999**, 2303−2304.
(20) Ossipoff, N. J.; Cant, N. W. *J. Catal.* **1994**, *148*, 125−133.
(21) Koeppel, R. A.; Wehrli, J. T.; Wainwright, M. S.; Trimm, D. L.; Cant, N. W. *Appl. Catal. A* **1994**, *120*, 163−177.

10.1021/cm021741x CCC: $25.00 © 2003 American Chemical Society
Published on Web 05/29/2003

of the composite and are therefore a sensitive function of the preparation method, particularly the drying method.[19] There appears to be a critical particle size for the catalyst: highly dispersed copper is largely unreactive, as are the large sintered aggregates that can form during catalyst activation and/or under reaction conditions (e.g., during reduction of CuO to Cu). The ideal catalyst would have small (nanoscale) uniform copper particles evenly distributed over a high surface area substrate. Velarde-Ortiz et al.[24] and Zhang et al.[25] have used dendrimers and microemulsion methods, respectively, coupled with sol−gel chemistry to control the size and distribution of copper or copper oxide particles in dense silicas.[22] Alternatively, because of the absence of ternary phases in the $CuO-SiO_2$ composition diagram, copper oxide particles can be formed from phase segregation by annealing silica samples containing dispersed copper. The introduction of copper is usually achieved either by impregnation of silica substrates with copper salts or by copolymerization of copper salts with silica sols. Toupance et al. have studied the effects of different impregnation methods and annealing and reduction conditions on the resultant copper particle size and polydispersity using commercial silica substrates.[26] They determined that the most important factors for obtaining small particles were the drying step and the strength of the binding of Cu^{2+} to the support.[19] Cordoba et al. employed sol−gel copolymerization methods followed by annealing for the formation of CuO/SiO_2 composite materials of varying CuO concentration.[27] They observed the presence of both dispersed Cu(II) and clustered Cu(II) (i.e., CuO clusters), with the latter dominating as the CuO concentration was increased above 0.5 mol %.

For specific studies on aerogels, the most extensive to date is that of Buckley and Greenblatt, who conducted a comparative study of silica alcogels (having an alcohol gel matrix), aerogels (produced by supercritical removal of alcohol), and xerogels (conventionally dried dense gels) that were doped with transition metal complexes and salts of Ni, Co, and Cu and subsequently annealed to 500 °C.[22] They also explored the copper speciation as a function of synthetic conditions (copolymerization vs impregnation) using electron paramagnetic resonance (EPR). The presence of Cu^{2+} in many of the unannealed samples was confirmed, and Cu^{2+} was found to be freely dispersed in the pore liquid (i.e., not bound to the silica surface). More recently, Hair et al. used copolymerization followed by supercritical CO_2 extraction for CuO/silica aerogel formation.[14,16] This "cold" extraction method is known to be more effective for maintaining the silica structure during removal of solvent than the "hot" supercritical removal of alcohol.[24] Not surprisingly, the surface areas of the Hair et al. samples are notably larger than those of Buckley and Greenblatt (~600 vs ~350 m^2/g); however, only a limited range of synthetic conditions and annealing treatments were investigated.

The potential of cold methods to produce aerogels with high surface areas, well-dispersed CuO, and good thermal stability warrants a more detailed study. In this report, we present a systematic study of the effects of the precursor salt, pH, and annealing temperature on the homogeneity, morphology, copper speciation, crystallinity, and surface area of ca. 3 wt % CuO in SiO_2 aerogels doped by copolymerization techniques and dried by the supercritical extraction of CO_2. For the purpose of comparison, conventionally dried gels (xerogels) are also analyzed.

Experimental Section

I. Preparation of Materials. Six different copper salts were examined as precursors for the incorporation of copper into silica: copper(I) chloride (99%, Acros), copper(II) chloride (anhydrous, 99%, Acros), copper(I) acetate (CuOAc, 97%, Aldrich), copper(II) acetate [$Cu(OAc)_2$, anhydrous, Acros], copper(II) sulfate (anhydrous, 99.7%, Fisher), and copper(II) nitrate (hydrate, 99.999%, Aldrich). Other chemicals, including methanol (MeOH), ammonium hydroxide, hydrochloric acid, potassium hydrogen phthalate (KHP), acetonitrile, and sodium hydroxide, were purchased from Fisher; tetraethyl orthosilicate (TEOS, 98%) was purchased from Acros; and tetramethyl orthosilicate (TMOS, 98%) was purchased from Alfa-Aesar. All chemicals were used as received. The following sections elaborate the synthetic procedures for each of the copper salts.

Gel Formation. (A) $Cu(OAc)_2$ Precursor. In the acid-catalyzed approach, 0.182 g of $Cu(OAc)_2$ was added to 9.00 mL of a solution of pH 4.6 KHP/NaOH buffer (0.05 M), and the resulting mixture was sonicated for 15 min. Another solution was prepared by mixing 5.20 mL of TMOS, 1.09 mL of water, and 0.07 mL of 0.04 N HCl. The two solutions were combined, mixed for 1 min, and stored in 5-mL polyethylene vials at room temperature for gelation. In the base-catalyzed approach, 0.137 g of $Cu(OAc)_2$ was dissolved in a mixture of 4.50 mL of MeOH, 1.50 mL of water, and 0.01 mL of 30% NH_4OH. This precursor solution was added to a mixture of 4.00 mL of TMOS and 4.50 mL of MeOH, and the resulting solution was mixed and transferred to 5-mL polyethylene vials.

(B) CuOAc Precursor. In this acid-catalyzed procedure, 17.74 mL TEOS was added to a mixture of 1.44 mL of H_2O, 4.5 mL of EtOH, and 0.02 mL of concentrated HCl, and the resulting solution was stirred for 30 min. In a separate beaker, 0.272 g of CuOAc was dissolved in 20 mL of EtOH, and then 0.015 mL of concentrated HCl was added. The copper precursor solution was then added to the hydrolyzed TEOS solution, and the mixture was stirred for 1 h. To complete the hydrolysis process, a mixture of 5.76 mL of H_2O, 4.5 mL of EtOH, and 0.07 mL of concentrated HCl was added to the above solution, and the resulting mixture was stirred for 30 min. The sol was then transferred to polyethylene vials for gelation.

(C) $CuCl_2$ Precursor. In this base-catalyzed synthesis, 0.327 g of $CuCl_2$ dissolved in 5 mL of MeOH was added to a mixture of 10 mL of TMOS and 4.5 mL of MeOH, and the resulting solution was mixed for 1 min. A 1.5-mL aliquot of H_2O was added to the mixture, the resulting solution was stirred for 1 min, and then 0.015 mL of 30% NH_4OH was added with mixing. The resulting sol was placed in a polyethylene vial for gelation.

(D) CuCl Precursor. In this base-catalyzed procedure, a solution of 17.74 mL of TMOS and 4.5 mL of MeOH was combined with another solution of 4.5 mL of MeOH, 1.5 mL of H_2O, and 0.010 mL of 30% NH_4OH. A solution of 0.337 g of CuCl dissolved in 10 mL of CH_3CN was added dropwise to this mixture . The resulting mixture was stirred for 5 min and then transferred to 5-mL polyethylene vials for gelation.

(22) Guerreiro, E. D.; Gorriz, O. F.; Larsen, G.; Arrúa, L. A. *Appl. Catal. A* **2000**, *204*, 33−48.
(23) Marchi, A. J.; Fierro, J. L. G.; Santamaría, J.; Monzón, A. *Appl. Catal. A* **1996**, *142*, 375−386.
(24) Velarde-Ortiz, R.; Larsen, G. *Chem. Mater.* **2002**, *14*, 858−866.
(25) Zhang, K.; Chew, C. H.; Xu, G. Q.; Wang, J.; Gan, L. M. *Langmuir* **1999**, *15*, 3056−3061.
(26) Toupance, T.; Kermarec, M.; Louis, C. *J. Phys. Chem. B* **2000**, *104*, 965−972.
(27) Cordoba, G.; Arroyo, R.; Fierro, J. L. G.; Viniegra, M. *J. Solid State Chem.* **1996**, *123*, 93−99.

(E) $CuSO_4$ Precursor. In this acid-catalyzed synthesis, 17.74 mL of TEOS was added to a mixture of 1.44 mL of H_2O, 4.50 mL of EtOH, and 0.02 mL of concentrated HCl, and the resulting mixture was stirred for 30 min. The $CuSO_4$ precursor (0.354 g) was dissolved in 13 mL of CH_3CN and added to the above mixture, and the combined solution was stirred for 1 h. Another solution of 5.76 mL of H_2O, 4.5 mL of EtOH, and 0.07 mL of concentrated HCl was added to the mixture, and the resulting solution was stirred for 30 min to complete the hydrolysis process. The green colored sol was placed in a polyethylene vial for gelation.

(F) $Cu(NO_3)_2$ Precursor. This acid-catalyzed synthesis is identical to that employed for $CuSO_4$ (E) but uses 0.417 g of $Cu(NO_3)_2$ dissolved in 13 mL of CH_3CN.

Gel Processing (All Salts). Gels (acid- and base-catalyzed) were aged overnight to increase gel firmness. For aerogel production, gels were exchanged with acetone 6−8 times over 2 days and then transferred, under acetone, to a SPI-DRY model critical point dryer, where they were subsequently washed and immersed in CO_2(l) for 1 h. To prevent formation of the base-catalyzed enol tautomer of acetone as a byproduct, base-catalyzed gels were initially washed with ethanol (4 times, every 2 h) prior to acetone exchange.[13,18] The CO_2(l) exchanged gels were dried under supercritical conditions by raising the drier temperature to 40 °C and maintaining this temperature for 30 min, and then CO_2 gas was vented over 45 min to obtain monolithic aerogels. For a comparative study, sets of xerogels were prepared by drying the wet gel conventionally (benchtop drying). Both xerogels and aerogels were placed in a preheated furnace and annealed at 400, 650, and 900 °C in air for 2 h to produce the copper oxide/silica composites.

II. Characterization. *Density Measurements.* Annealed monolithic gels were weighed, and the bulk density was calculated from this mass and the cylindrical volume of the monolith.

Scanning Electron Microscopy (SEM). SEM images were obtained at 25 keV in secondary-electron mode using a Hitachi S-2400 microscope. Dried gel samples were spread on carbon adhesive tabs on an SEM stub and coated lightly with Au using a Au evaporator setup.

Transmission Electron Microscopy (TEM). TEM analyses were conducted in bright-field mode at the Electron Microscopy Analysis Lab (EMAL), University of Michigan, using a JEOL 4000EX microscope at an accelerating voltage of 400 keV. Fine powders of annealed samples were dispersed in acetone with sonication and placed on a holey carbon coated grid by dipping the grid into the solution and subsequently evaporating the acetone.

Powder X-ray Diffraction. A Rigaku Ru 200B X-ray diffractometer (40 kV, 100 mW, Cu Kα radiation) with a rotating anode was employed for X-ray powder diffraction measurements. Powder samples were placed on double-stick tape and covered with transparent tape for the analyses. Samples were identified by comparison to phases in the ICDD powder diffraction file (PDF) database (release 2000). CuO particle size calculations were performed using the Scherrer equation.[28]

Surface Area Analysis. A Micromeritics model ASAP 2010 surface area porosimeter was used to obtain nitrogen physisorption isotherms at 77 K. Surface areas were evaluated using the Brunauer−Emmett−Teller (BET) model for data points between reduced relative pressure values of 0.05 and 0.20 and assuming the area occupied by a nitrogen molecule to be 16.2 Å^2. Average pore diameters and pore volumes were calculated using the adsorption branch of the isotherm in the Barrett−Joyner−Halenda (BJH) equation, and pore size distributions were determined from density functional theory (DFT) modeling. Before each set of measurements, powder samples were degassed for 18−26 h at 300 °C. Each measurement took ca. 24 h to complete with a 10-s equilibrium interval.

X-ray Fluorescence (XRF) Analysis. A wavelength-dispersive Siemens model SRS 300 spectrometer with a Cu target (40 kV, 30 mA) was used to obtain both qualitative and quantitative measurements on doped aerogels and xerogels. The copper quantification was obtained on glass beads prepared from lithium tetraborate fluxes of xerogel and aerogel samples using a LiF(200) detector in the range 38−58° 2θ.[29] A set of copper concentration standards was produced and run under identical conditions.

Electron Paramagnetic Resonance (EPR) Analysis. Powder samples were placed in quartz tubes and analyzed at 130−140 K using a Bruker EMX model EPR spectrometer at 9.43 GHz (X-band) microwave frequency. The following parameters were employed for each scan: 4 G modulation amplitude, 10 mW microwave power, 81.92 ms conversion time, and 327.68 ms time constant.

Results

Synthesis. A variety of copper salts were explored for their feasibility in copper oxide/silica composite aerogel formation via copolymerization sol−gel processing. CuOAc, $Cu(OAc)_2$, CuCl, $CuCl_2$, $CuSO_4$, and $Cu(NO_3)_2$ were treated with tetraethyl or tetramethyl orthosilicate (TEOS or TMOS) under acid- and/or base-catalyzed conditions, exchanged with acetone, and then supercritically dried with CO_2 to obtain monolithic aerogels. Where salts demonstrated poor solubility in aqueous alcohol, acetonitrile was used to introduce the copper into the sol. In each case, a nominal CuO concentration of 3 wt % was targeted. Both CuOAc and $CuSO_4$ (acid catalyzed) and $CuCl_2$ and CuCl (base catalyzed) produced transparent green gels, but the CuCl gel deposited a blue precipitate over time. All four gels lost significant quantities of copper (observed as color loss) during the acetone wash step. Gels of $Cu(NO_3)_2$ produced under acid-catalyzed conditions were blue and likewise lost nearly 75% of their copper content during the exchange step. For $Cu(OAc)_2$, a transparent, blue-colored composite wet gel was obtained over 20−30 min in acid-catalyzed systems and 1.5 days in base-catalyzed systems. In both cases, the wet gels were robust, and little or no precipitates were found by SEM analysis. Some loss of copper during solvent exchange was evident in acid-catalyzed $Cu(OAc)_2$ gels by the coloration of the acetone wash solvent. No such loss was apparent in the analogous base-catalyzed gels. Compared to all of the other precursors examined here, the loss of Cu^{2+} during washing was minor for $Cu(OAc)_2$. Accordingly, the rest of the study was conducted only on composite gels derived from $Cu(OAc)_2$.

Dried Gels with $Cu(OAc)_2$ Precursor. Aerogels recovered after supercritical fluid extractions were monolithic and deep blue in color. Compared to xerogel counterparts having 70−80% volume loss, aerogels showed little or no change in volume when compared to the wet gel precursor. The specific concentration of Cu was determined by quantitative XRF analysis and found to range from 1.9 to 2.4% (see Table 1). However, there was a noticeable decrease in copper content in aerogels relative to xerogels, and this change was more drastic for the acid-catalyzed aerogels than for those that were base catalyzed.

(28) Cullity, B. D. *Elements of X-ray Diffraction*, 3rd ed.; Prentice Hall: Upper Saddle River, NJ, 2001.

(29) Buhrke, D. K., Jenkins, R., Smith, D. K., Eds. *A Practical Guide for the Preparation of Specimens for X-ray Fluorescence and X-ray Diffraction Analysis*; Wiley & Sons: New York, 1998.

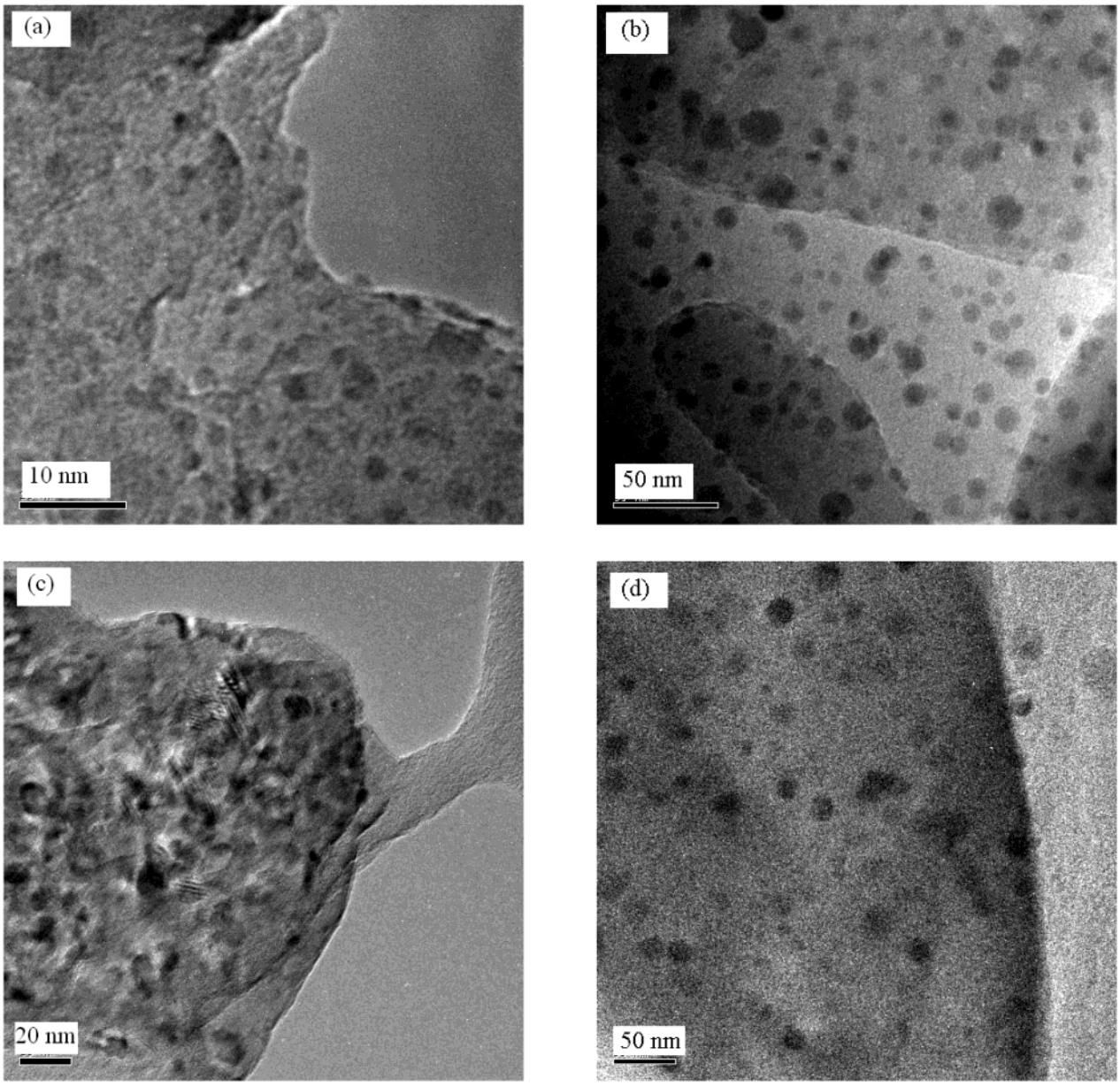

Figure 1. TEM images of air-annealed CuO/silica composite xerogels: (a) acid catalyzed, 650 °C; (b) base catalyzed, 650 °C; (c) acid catalyzed, 900 °C; (d) base catalyzed, 900 °C.

Table 1. Copper Concentration via Quantitative XRF Analysis[a]

doped gels	CuO (wt %)	Cu (wt %)
acid-catalyzed xerogel	3.06	2.44
acid-catalyzed aerogel	2.41	1.93
base-catalyzed xerogel	2.92	2.33
base-catalyzed aerogel	2.78	2.22

[a] Target CuO = 3 wt %.

CuO Formation. To examine the effect of temperature on the formation and distribution of CuO particles within the silica matrix, xerogels and aerogels were annealed at 400, 650, and 900 °C in air for 2−3 h. Transmission electron micrographs of CuO/silica xerogels are shown in Figure 1a−d as a function of annealing temperature and synthetic conditions (acid or base catalyzed). Segregated CuO shows up as regions of high contrast in the electron micrographs. In the case of both acid- and base-catalyzed xerogels, copper oxide nanoparticles are first observed in samples annealed at 650 °C (Figure 1a and b) and are still present upon 900 °C annealing (Figure 1c and d). Indeed, at 900 °C, the acid-catalyzed xerogel has a significant crystalline fraction, as evidenced by the presence of Fresnel fringes (Figure 1d). Aerogels, on the other hand, do not show the presence of segregated CuO until they are annealed at 900 °C (Figure 2a−d). In all cases (aerogels and xerogels), the CuO particles produced show a large degree of polydispersity (size range of 5−50 nm), with larger particles observed in acid-catalyzed samples (aerogels).

Powder X-ray diffraction (PXRD) analyses were employed to determine the temperature at which crystallization of the composite commences. PXRD measurements of 400 and 650 °C annealed (in air) acid- and base-catalyzed xerogels and aerogels result in amorphous spectra. However, in samples annealed at ≥900 °C, peaks corresponding to crystalline CuO (tenorite) can be clearly seen (Figures 3 and 4). From the aerogel spectra, base-catalyzed samples have broader peaks

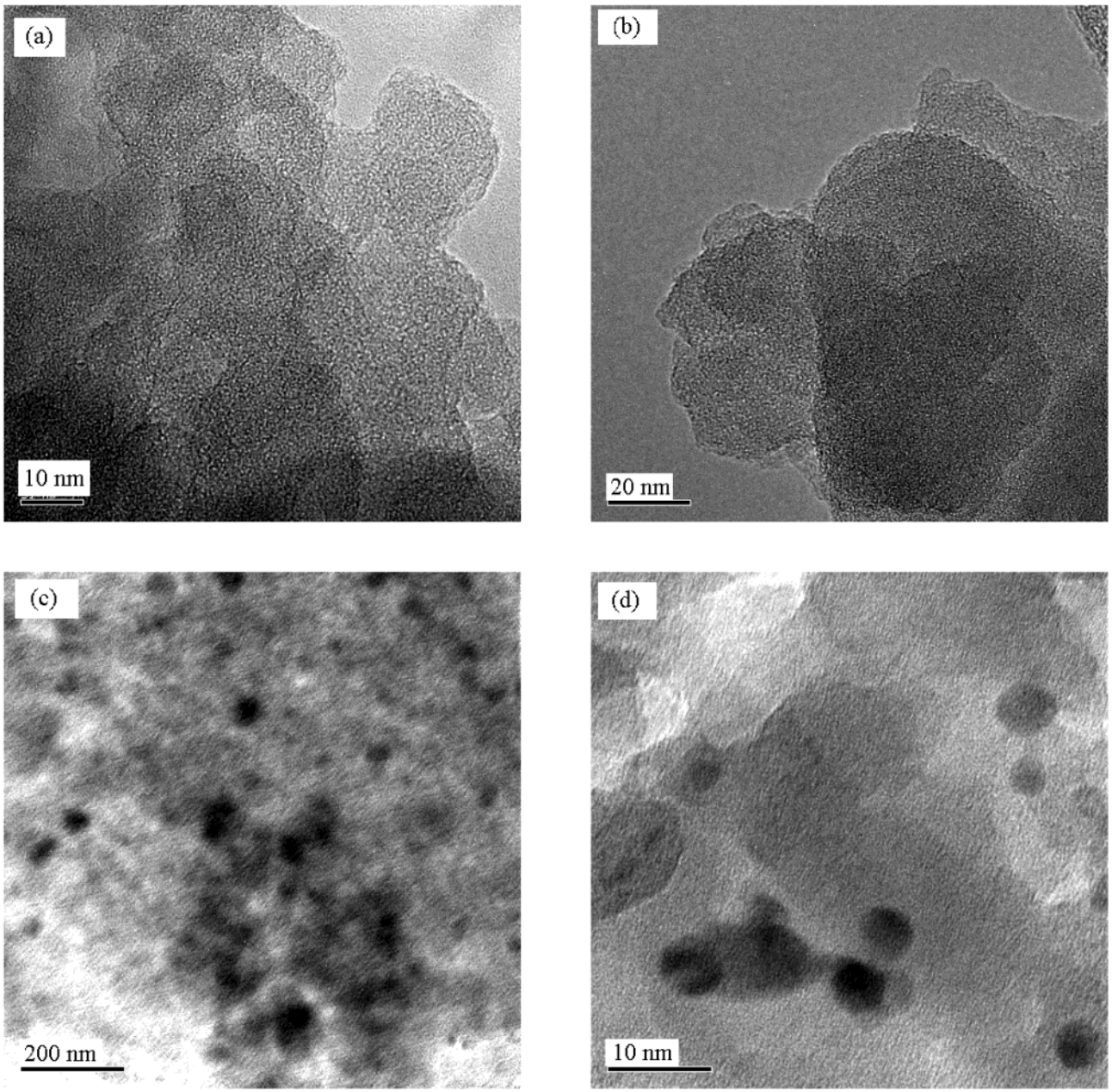

Figure 2. TEM images of air-annealed CuO/silica composite aerogels: (a) acid catalyzed, 650 °C; (b) base catalyzed, 650 °C; (c) acid catalyzed, 900 °C; (d) base catalyzed, 900 °C.

than acid-catalyzed samples. Particle size analysis using the Scherrer equation[28] shows that the average CuO particle size is ∼26 and ∼15 nm in acid- and base-catalyzed aerogels, respectively. The acid- and base-catalyzed xerogel spectra also indicate the presence of crystalline silica as crystobalite and quartz, respectively (Figure 3).

Surface Area Analyses. All of the aerogel samples analyzed show a type IV isotherm characteristic of mesoporous materials (pore size of 2−50 nm), and xerogels show a type I isotherm characteristic of microporous materials (<2 nm).[13] A comparison of the adsorption/desorption isotherms of acid- and base-catalyzed composite xerogels and aerogels annealed at 650 °C is shown in Figure 5, and the results of analyses at all three temperatures are presented in Table 2. There is a substantial increase in surface area, average pore diameter, and total pore volume for composite aerogels relative to their conventionally dried (xerogel) counterparts for both the acid- and base-catalyzed cases. In addition, the insets of Figure 5 show that the pore size distribution among copper oxide/silica composite xerogels and aerogels are fully consistent with the isotherm shapes: aerogels have a wider pore distribution and are largely mesoporous, whereas xerogels have a narrower pore distribution with mostly micropores.

Compared to the plain silica aerogel counterparts, the surface areas and total pore volumes of the acid- and base-catalyzed copper oxide/silica composite aerogels have increased considerably (see Table 2; isotherms and pore size distribution shown in Figure 6). However, the average pore diameter actually decreases for the composite aerogels relative to the plain silica (Table 2). This is evident from the insets of Figure 6, where acid-catalyzed composite aerogels show a narrow peak in the pore size distribution with a sharp cutoff at around 200

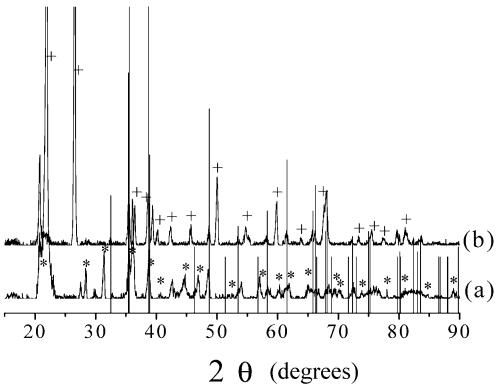

Figure 3. Powder X-ray diffraction patterns of (a) acid-catalyzed and (b) base-catalyzed CuO/silica xerogels annealed at 900 °C for 2 h. The PDF overlay of CuO (48-1548) is shown in both cases as vertical line drops, and peaks labeled with asterisks (*) and crosses (+) correspond to the crystobalite (39-1425) and quartz (46-1045) polymorphs of SiO_2, respectively.

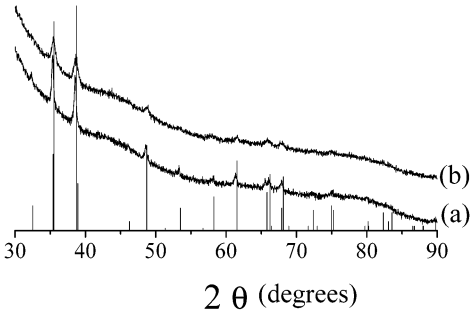

Figure 4. Powder X-ray diffraction patterns of (a) acid-catalyzed and (b) base-catalyzed CuO/silica aerogels annealed at 900 °C for 2 h. The PDF overlay of CuO (48-1548) is shown as vertical line drops.

Table 2. BET Surface Areas, BJH Adsorption Average Pore Diameters, and BJH Adsorption Total Pore Volumes for Silica Aerogels and Copper Oxide Doped Silica Xerogels and Aerogels[a]

	surface area (m^2/g)		average pore diameter (Å)		total pore volume (cm^3/g)	
	AC	BC	AC	BC	AC	BC
			SiO_2 aerogel			
400 °C	553	784	105	128	1.49	1.96
650 °C	502	538	113	134	1.53	1.51
900 °C	154	435	106	166	0.43	1.74
			CuO_x/silica aerogel			
400 °C	831	923	87	116	1.62	2.20
650 °C	562	753	87	111	1.27	1.99
900 °C	68	338	221	127	0.34	1.12
			CuO_x/silica xerogel			
650 °C	354	352	32	26	0.23	0.17

[a] AC = acid catalyzed, BC = base catalyzed.

Å, relative to a broader peak in the plain aerogel stretching out to >300 Å. For the base-catalyzed samples, the plain aerogels have a single peak in the pore size distribution from 200 to 500 Å, but this is superimposed on a second peak in the 10−300 Å region (i.e., a bimodal distribution) for the composite.

Increasing the annealing temperature decreases the surface area and total pore volume and increases the average pore diameter in both plain and copper oxide composite silica aerogels. These variations are more apparent in gels that are annealed at 900 °C (see Table 2).

Table 3. Bulk Density Measurements of CuO/SiO_x Gels (in cm^3/g)

	unannealed	400 °C	650 °C	900 °C
AC aerogel	0.353	0.504	0.515	1.06
BC aerogel	0.465	0.483	0.542	0.630
AC xerogel	1.06	–	–	–
BC xerogel	1.39	–	–	–

It should be noted that, although plastic deformation is a concern in compliant materials such as aerogels, we addressed this issue by using an equilibrium interval greater than that reported for monolithic samples[30] and measuring powder samples (as opposed to monoliths) for consistency. We also conducted density measurements (Table 3), which show that the aerogel pore volume decrease, as determined by BJH analysis, is a result of densification upon annealing.

Electron Paramagnetic Resonance (EPR) Analysis. EPR analyses were undertaken to elucidate the speciation of copper in the aerogel and xerogel materials. Room-temperature EPR analyses of unannealed acid (washed and unwashed) and base-catalyzed copper/silica composite xerogels are presented in Figure 7. In all cases, there is an axial signal with hyperfine splitting clearly resolved only for the parallel component ($g_{||}$) and a hyperfine splitting constant of $140-150 \times 10^{-4}$ cm^{-1}. However, for unwashed acid-catalyzed xerogels, the splitting patterns are asymmetric and diffused or consist of two patterns overlapped (Figure 7b) and do not clearly resolve until after washing. No apparent difference is observed in the EPR spectra of base-catalyzed composite xerogels that are washed with acetone or remain unwashed. The aerogels are virtually identical to their xerogel counterparts, except for a sharp peak at 3363 G (see Figure 8) corresponding to $g = 2.0037$.

EPR spectra of room temperature and air-annealed composite xerogels and aerogels are shown in Figure 8, along with the isotropic, nearly featureless spectrum of bulk CuO for comparison (upper right-hand corner). All unannealed gels have g factors of 2.07−2.08. For acid-catalyzed samples, very little change is observed in the EPR spectra for xerogel samples heated at 400 or 650 °C relative to room-temperature samples. However, the 900 °C sample appears to have a broad, isotropic contribution to the signal superposed over the individual $g_\perp$ and $g_{||}$ components. Aerogels show a substantial change between 25 and 650 °C, where the perpendicular component loses prominence (i.e., is broadened) as the low-intensity hyperfine ($g_{||}$) features overlap with the $g_\perp$ component. Although this broadening effect is also present in the 900 °C annealed aerogel sample, the signal intensity of the perpendicular component is recovered. Moreover, the signal shape anisotropy is considerably different in the 900 °C annealed acid-catalyzed aerogel sample compared to the xerogel analogue. For base-catalyzed samples, the xerogels and aerogels are very similar. Upon heating, the hyperfine splitting of the parallel component becomes increasingly broadened ($\Delta A_{||} \approx 23 \times 10^{-4}$ cm^{-1}) with a nonuniform distribution of intensity. Moreover, in base-catalyzed aerogels, a higher degree of nonsymmetric broadening is observed with annealing temperature. By 900 °C,

(30) Reichenauer, G.; Scherer, G. W. *J. Non-Cryst. Solids* **2001**, *285*, 167−174.

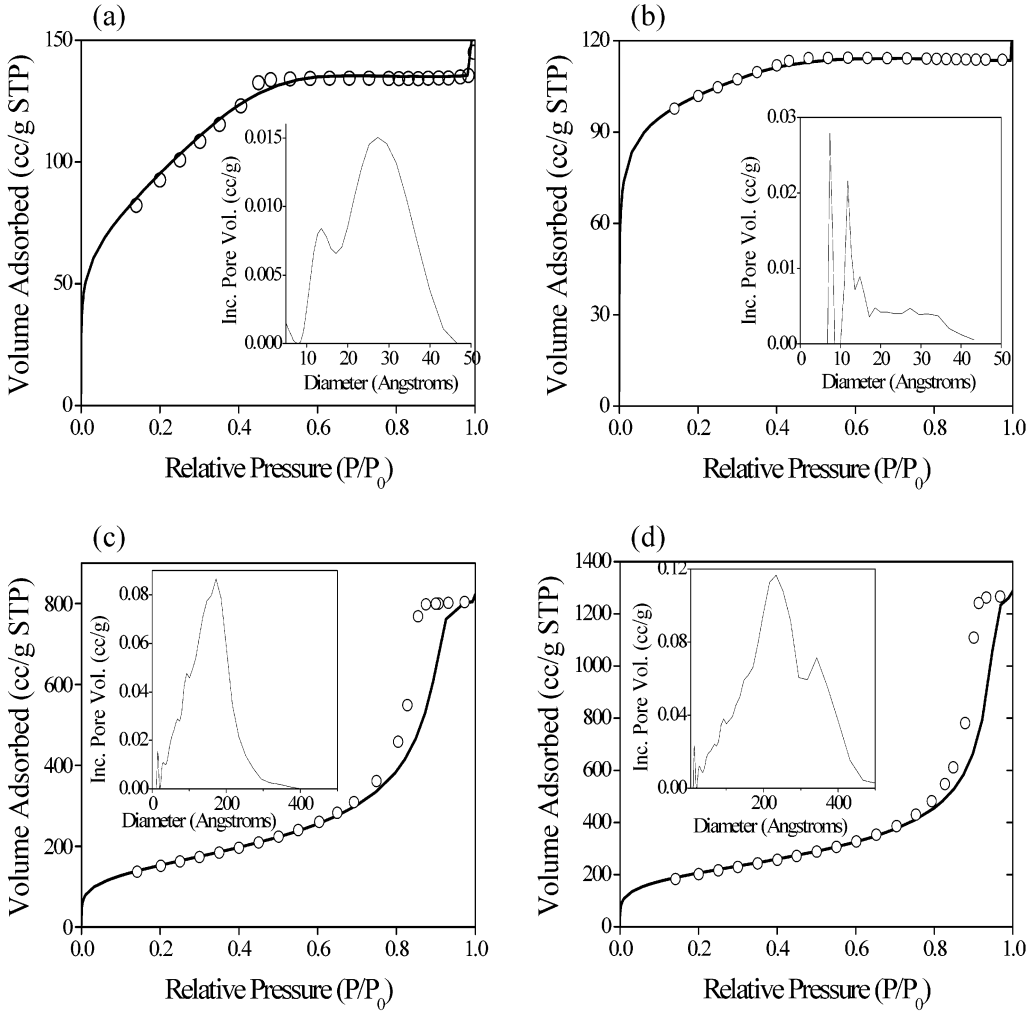

Figure 5. Nitrogen adsorption (—) and desorption (○) isotherms of CuO/silica xerogels at 77 K [(a) acid catalyzed, (b) base catalyzed] and of CuO/silica aerogels [(c) acid catalyzed, (d) base catalyzed], all annealed at 650 °C. The inset shows the pore distribution calculated using density functional theory and assuming a slit geometry.

there is a significant isotropic contribution to the signal. Although a similar broadening effect with respect to $g_\perp$ is observed in base-catalyzed xerogels, the $g_{||}$ hyperfine splittings appear to be more abrupt and nonuniform.

Discussion

Copper Binding within the Silica Matrix. One of the most important criteria for CuO/silica aerogel composite formation via cold SCE methods is the binding of Cu to the SiO_2 matrix. To successfully "dry" the gels without pore wall collapse, the aqueous alcohol solution in the pores must first be replaced with a solvent in which CO_2(l) has greater miscibility, such as acetone. Complexes that bind poorly to the silica can be washed away during this step, resulting in decreased Cu loading in the aerogel material.

The axial nature of the room-temperature EPR spectrum of the unannealed composite xerogel prepared with $Cu(OAc)_2$ is consistent with copper (Cu^{2+}) species bound to the silica. The four line splitting is due to the hyperfine coupling of ^{63}Cu and ^{65}Cu with the unpaired electron and is consistent with an axially distorted octahedron about the copper species due to a Jahn–Teller distortion in which the electron resides in the $d_{x^2-y^2}$ orbital. The g factors ($g_\perp = 2.07-2.08$) and hyperfine splitting constants ($A_{||} = 140-150 \times 10^{-4}$ cm^{-1}) are also consistent with oxygen coordination in a distorted octahedral environment,[15] and the increased broadening of the line width as a function of increasing m_I is expected for the glassy environment because of fluctuations in ligand field and bond covalencies.[31] An analogous axial spectrum (room temperature, Figure 8a and b) of an unannealed composite aerogel indicates that adhered copper species are preserved even after supercritical drying. This is consistent with the fact that most of the copper is retained during the washing step, as evidenced qualitatively by color retention and quantitatively by XRF.

There are some discrepancies between acid-catalyzed (AC) and base-catalyzed (BC) systems. The room-temperature EPR spectrum of the unwashed acid-catalyzed xerogel shows an asymmetric, diffuse hyperfine splitting pattern ($g_{||}$), leading us to believe that a second isotropic, unbound component might be present. At room temperature, broad, isotropic signals are observed when tetragonally distorted Cu species are present in the pore solution, where the molecular motion of the Cu^{2+} ion is much faster than the EPR time

(31) Darab, J. G.; MacCrone, R. K. *Phys. Chem. Glasses* **1991**, *32*, 91–102.

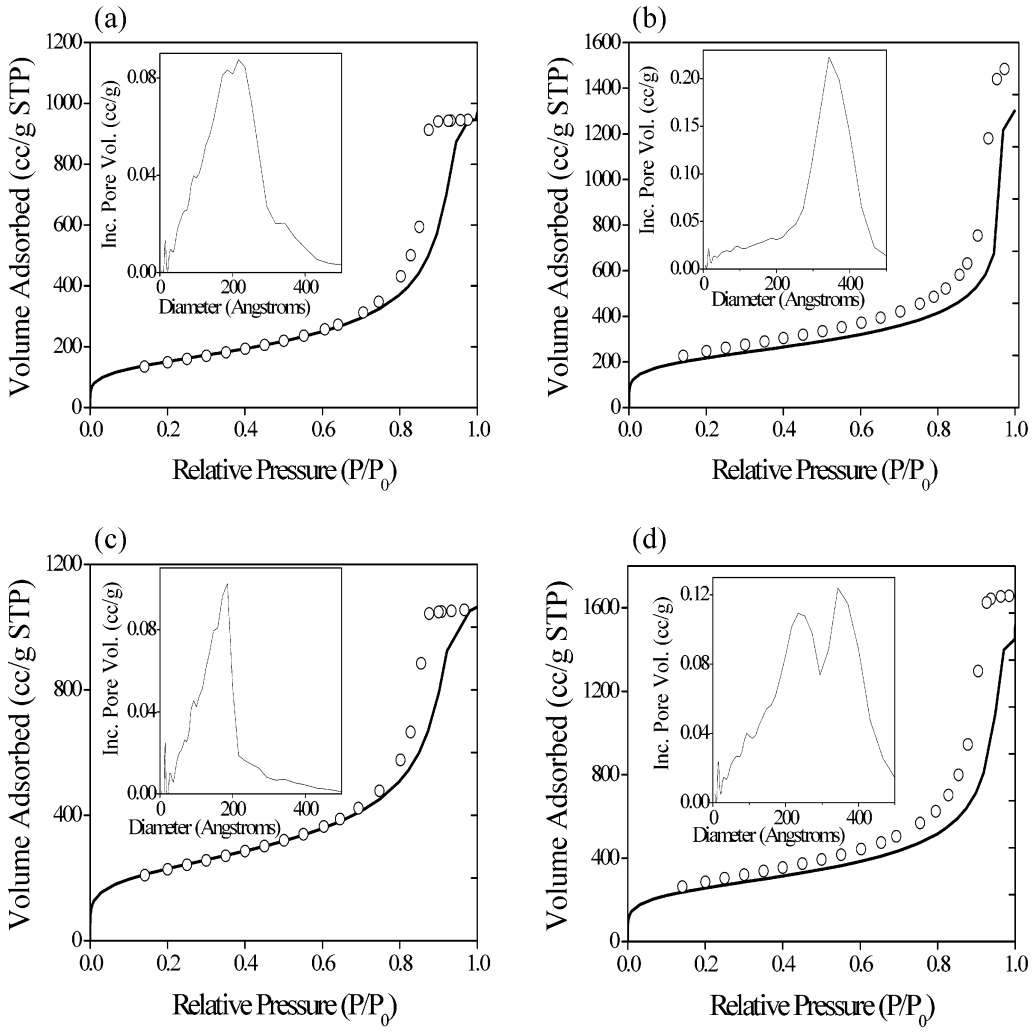

Figure 6. Nitrogen adsorption (—) and desorption (○) isotherms of plain silica aerogels [(a) acid catalyzed, (b) base catalyzed] and of CuO/silica aerogels [(c) acid catalyzed, (d) base catalyzed], all annealed at 400 °C. The inset shows the pore distribution calculated using density functional theory and assuming a slit geometry.

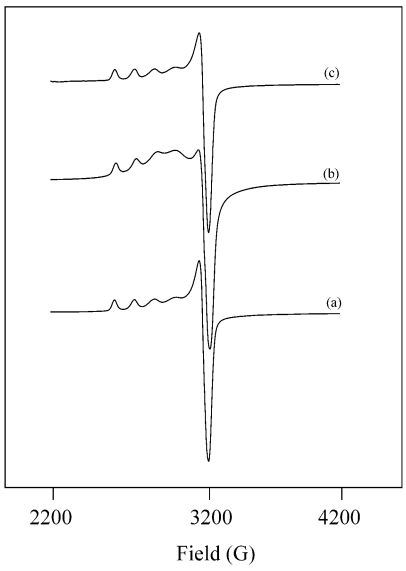

Figure 7. Room-temperature EPR spectra of (a) base-catalyzed CuO/silica xerogel, unwashed; (b) acid-catalyzed CuO/silica xerogel, unwashed; and (c) acid-catalyzed CuO/silica xerogel, washed.

scale.[15,31] Upon washing, the AC xerogel pattern resolves into a single axial component (also observed for the BC xerogel), suggesting that the unbound copper present in the pore liquid has been removed. The presence of the small isotropic component in the AC xerogel is consistent with greater Cu losses in this system, as observed in the coloration of the acetone wash, and lower overall copper incorporation by XRF. The sharp feature present in both aerogels (but most evident in the AC system) is likely due to some kind of a radical species (g = 2.0037) produced during the supercritical extraction.[31,32] The g factor of the radical species is consistent with that of a free electron (g = 2.0023). This feature disappears upon annealing.

The mechanism of the binding of copper(II) acetate within the silica matrix remains unresolved, but we speculate it might result from bridging acetate functionalities. Indeed, because SiO_2 and CuO do not form a glass, the complete removal of ligands from the copper precursor during the sol−gel reaction is expected to lead to a heterogeneous material, i.e., thermodynamically, Si−O−Si and Cu−O−Cu are favored over Si−O−Cu. In fact, this is eventually achieved through thermal treatment of the aerogels, resulting in nucleation of CuO within the silica matrix. Careful analysis of wet gels

(32) Duval, E.; Bovier, C.; Roux, H.; Serughetti, J.; Tuel, A.; Wicker, G. *J. Non-Cryst. Solids* **1995**, *189*, 101−106.

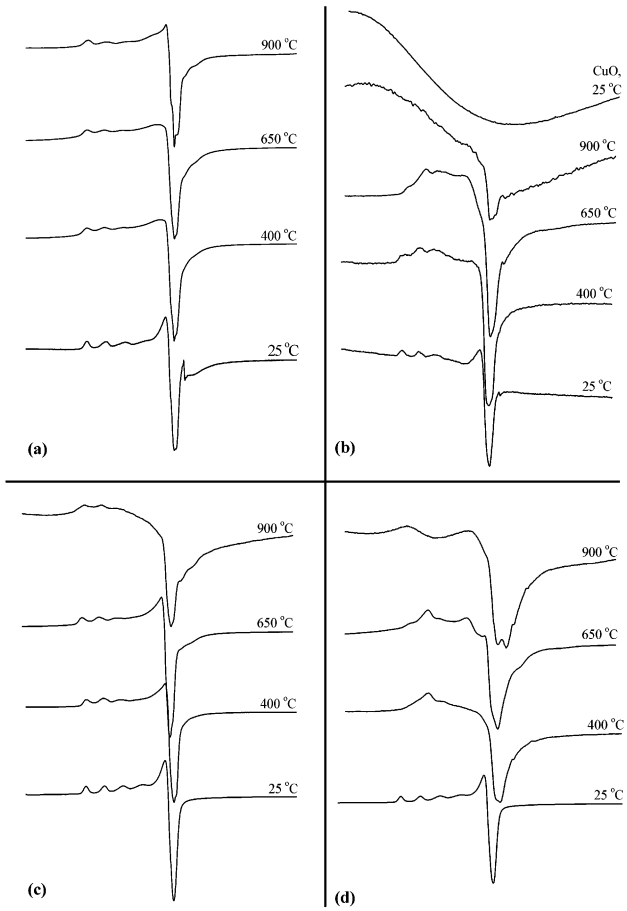

Figure 8. Low-temperature (130−140 K) EPR spectra of (a) acid-catalyzed aerogels; (b) base-catalyzed aerogels; (c) acid-catalyzed xerogels, washed; and (d) base-catalyzed xerogels, unwashed, all annealed at the indicated temperatures. The spectrum of bulk CuO is shown for comparison in the upper right-hand corner.

shows that precipitation is common on the microscale for salts other than $Cu(OAc)_2$, and loss of color during the exchange process was found for CuCl, $CuCl_2$, $CuSO_4$, $Cu(NO_3)_2$, and, to a lesser extent, CuOAc. Among the complexes assayed, the best in terms of homogeneity and binding strength was found to be copper(II) acetate in which the copper has already adopted the oxidation state in which it is most stable in aqueous solution and is paired with a ligand (acetate) capable of bridging two metals (e.g., Cu−Si). Preliminary evidence from gels synthesized under the same conditions using a $Cu(acac)_2$ precursor reveals that Cu is again bound to the silica network, although minor losses are observed in the acetone exchange step, as in the $Cu(OAc)_2$ system. Mayo et al. suggested that the Cu in $Cu(acac)_2$ might act as a template for silica gel formation via a bridging $Cu\text{-}(O\text{-}Si)_x$ intermediate that brings together multiple siloxy groups.[33] However, judging from the poor adhesion of most of the copper salts assayed, we believe it far more likely that the bidentate ligand (acac or OAc) takes an active role in tethering copper to silica and subsequently impacting gel formation. Greater losses (21% in AC vs 5% in BC) observed in AC systems might be due to acid-catalyzed hydrolysis of these purported binding acetate groups.

(33) Mayo, E. I.; Pooré, D. D.; Stiegman, A. E. *Inorg. Chem.* **2000**, *39*, 899−905.

Effect of Copper on Aerogel Formation. Generally, in acid-catalyzed samples, the complete removal of pore liquid is difficult, resulting in greater shrinkage and therefore lower surface areas than in base-catalyzed counterparts. This is because, under acidic conditions, polymer-like gels are favored, and these gels have smaller pores than the "pearl necklace" base-catalyzed colloidal gels,[10,13] thus inhibiting CO_2 diffusion during supercritical fluid extraction.[3] Our data are consistent with this general wisdom: AC aerogels have lower surface areas and smaller average pore sizes than BC aerogels, and both have considerably larger surface areas than their xerogel counterparts (see Figures 5 and 6 and Table 2). The addition of copper might be expected to disrupt the formation of a robust polymer lattice, resulting in collapse. However, for samples annealed at low temperatures (400 and 650 °C) the addition of Cu results in a dramatic increase in surface area relative to the plain silica counterparts. Thus, if copper is disrupting the polymeric lattice, the result would appear to be greater porosity. From the pore size distribution (Figure 6, insets), the effect of copper is to introduce a significant portion of smaller pores (ca. 200 Å) in addition to the larger (200−400 Å) pores observed in pure silica samples. Upon heating to 900 °C, the acetate groups have departed, and the CuO/SiO_x aerogels have densified considerably. Accordingly, the surface areas of the CuO/SiO_x aerogels drop well below those of pristine aerogels.

Copper Oxide Particle Formation. As a result of the fact that CuO and SiO_2 do not combine to form a glass or any discrete compounds, annealing of the homogeneous aerogel composites in air is expected to result in segregation of copper and concomitant formation of copper oxide nanoparticles that are embedded within the silica matrix. Consistent with the observations of other groups, annealing of our xerogels and aerogels does produce heterogeneous composites of CuO and SiO_2, as illustrated in the TEM data (Figures 1 and 2). However, we note a clear difference in the temperatures at which particle formation takes place. For the xerogels, particles are evident in samples annealed at 650 °C, whereas particles are not observed in aerogels until 900 °C, suggesting that the higher surface areas in the latter materials might be inhibiting segregation. Overall, the BC aerogel samples display smaller CuO particles in TEM images and broader peaks in XRD spectra (consistent with smaller crystallite size) than the AC analogues. Possibly, the relative rate of CuO particle nucleation is faster in BC samples, resulting in a greater number of nuclei and a correspondingly smaller size of those nuclei compared to AC samples. The ultimate result of CuO segregation is significant structural collapse, resulting in considerably lower surface areas relative to pure silica analogues and therefore greater losses than might be expected from mere thermal sintering.

The question of thermal sintering is not a simple one. Pure silica aerogels densify upon heating, and we observe a similar densification in the CuO/SiO_x aerogels (Table 3). However, Cu is known to promote crystallization in silica as well. For pure silica, crystallization is not expected to occur until 1300 °C, at which point

the crystobalite phase is favored.[34] With 3 wt % CuO in the gels, crystallization of silica is observed at 900 °C in xerogel samples (Figure 3), with crystabolite observed in AC samples and quartz in BC samples. These peaks are in addition to crystalline peaks corresponding to CuO. In aerogels, however, silica crystallization seems to have been retarded. The only crystalline phase present in both AC and BC aerogels is CuO (Figure 4). Despite the fact that segregated particles are observed in 650 °C annealed xerogels (Figure 1a,b), no crystalline pattern is observed by XRD. It might be that segregation occurs prior to crystallization. Indeed, the only sample in which a crystalline phase is implicated in the TEM is that of AC xerogels heated at 900 °C (Figure 1c), in which Fresnel fringes are clearly observed.

When comparing EPR spectra of base-catalyzed and acid-catalyzed composite xerogels and aerogels, distinct differences are observed because of the structural and compositional transformation of the copper species. In base-catalyzed gels, a gradual change from a well-resolved hyperfine pattern to a broadened, isotropic signal is observed as the annealing temperature is increased to 900 °C (Figure 8b,d). The broadening of the $g_{\perp}$ signal with increasing annealing temperature can be attributed to spin−lattice relaxation and to structural changes, in this case segregation of CuO.[15,26,31] At intermediate temperatures, the hyperfine features appear to be asymmetrical, suggesting multiple coordination environments of the copper ions. The absence of the hyperfine splittings ($g_{\parallel}$) and the large isotropic contribution observed in the 900 °C samples suggests that the Cu species is no longer immobilized (i.e., it becomes similar to bulk CuO). In contrast, AC aerogels and xerogels show the presence of hyperfine coupling even at 900 °C, suggesting that there is some component of axially distorted isolated copper ions under all conditions (Figure 8a,c). This is particularly interesting given that the aggregates and crystallites in AC gels appear to be considerably larger than those in BC gels. If nucleation proceeds at a lower rate in AC samples, it could be that the formation of fewer nuclei (which are, accordingly, larger) results in some of the Cu^{2+} species being effectively stranded away from these nuclei. As in BC systems, the intensity of the hyperfine peaks relative to an additional isotropic component decreases with increasing heating, consistent with aggregation of copper species to form CuO particles. The signal shape anisotropy and coexistence of isotropic and hyperfine signals as a function of temperature are due to the structural changes of the Cu^{2+} environment and gel pores. These findings are consistent with the literature.[31] It is interesting to note that the EPR data, which reflect the local environment of Cu^{2+}, appear to display a smooth transformation with increasing temperature, in contrast to the TEM and XRD data, which show clear cut-off temperatures for significant aggregation and crystallization, respectively, as well as a clear dependence on the overall surface area (aerogel vs xerogel).

(34) Battisha, I. K. *Egypt. J. Sol.* **2001**, *24*, 51−65.

Conclusions

We have conducted a systematic study of CuO/silica composite aerogels and xerogels and evaluated the effect of precursor salt, pH, and annealing temperature on the surface area, copper speciation, and crystallinity/particle size. Copper(II) acetate was found to be a superior precursor for the preparation of homogeneous copper-incorporated gels under both acidic and basic conditions relative to Cu(OAc), CuCl, $CuCl_2$, $CuSO_4$, and $Cu(NO_3)_2$. Upon annealing, the dispersed Cu^{2+} in the gels goes through a series of structural changes as the acetate group decomposes and Cu^{2+} segregates to CuO. On the basis of aggregate and crystallite size differences in aerogel species, we postulate that CuO nucleation might be faster in base-catalyzed systems than in acid-catalyzed systems, resulting in more nucleation and smaller particles overall. Although base-catalyzed gels undergo a gradual change from bound Cu^{2+} to segregated CuO with heating (25−900 °C), acid-catalyzed gels contain both species, even upon annealing at 900 °C, suggesting the presence of stranded Cu^{2+} species.

The composite aerogels exhibit higher surface areas than the plain silica analogues for unannealed samples as well as materials annealed up to 650 °C (increased microporosity). However, upon heating at 900 °C, the surface area of the composite rapidly plummets, concomitant with CuO aggregate formation. Nevertheless, the surface areas reported here (∼900 m^2/g) are substantially higher than those for other CuO/SiO_2 aerogels reported in the literature (∼350,[15] ∼600 m^2/g[14]).

Acknowledgment. We thank Dr. Corinna Wauchope and Dr. John Mansfield for their assistance with TEM analyses, Prof. David E. Benson for his insights into EPR data interpretation, Dr. Debra Rolison and Dr. Jeff Long for advice on aerogel preparation, Prof. Lowell Wenger for useful discussion and support, Mr. Greg Thiele for assistance with nitrogen adsorption isotherm interpretation, Dr. David A. Benson for training in sample preparation and measurement for quantitative XRF, and Ms. Marla Parson for preliminary work in this area. Financial support was provided by NSF IGERT (J.L.M.) and Research Corporation (Research Innovation Award-R10617).

CM021741X